

Modeling of hole-expansion of AA6022-T4 aluminum sheets with anisotropic non-quadratic yield functions

Yannis P. Korkolis¹, Benjamin Brownell¹, Sam Coppieters² and Haobin Tian³

¹U. of New Hampshire, USA

²KU Leuven, Technology Campus Ghent, Belgium

³Shanghai Second Polytechnic U., China

yannis.korkolis@unh.edu

Abstract. In the hole-expansion of anisotropic AA6022-T4 sheets, the strain around the hole is non-uniformly distributed due to the anisotropy of the material. This was examined by performing experiments with a flat-headed punch and using Digital Image Correlation (DIC). In the experiments, failure always initiated at a unique location, oriented at 45° to the Rolling Direction of the sheet. The use of DIC allowed the probing of the full-strain-field in real-time. Subsequently, the experiments were simulated in DYNAFORM using shell elements and the Yld2000-2D anisotropic non-quadratic yield function, properly calibrated for this material. In addition, the hardening curve of the material was inversely identified at large strains from the tail of the tensile test. The strain evolution is compared between the experiments and the model.

1. Introduction

The expansion of the circular hole of a thin sheet is a classical problem in plasticity [1]. Beyond its applications in assessing the performance of plasticity theories and in shedding light into the mechanics of material failure by void growth, it is also relevant to predicting splitting fractures in sheet metal forming and understanding the effect of edge preparation on sheet formability. In this study, we examine the hole-expansion of a plastically orthotropic sheet by a flat-headed punch [2], using a combination of experiments and analysis. The anisotropy and post-necking hardening response of the AA6022-T4 material of this study is first established experimentally. Subsequently, the hole-expansion experiments are described, including the use of Digital Image Correlation for real-time measurement of the strain fields. Finally, finite element simulations of hole-expansion using the commercial software DYNAFORM are presented and their predictions are compared to the experiments.

2. Material Modeling

The plastic anisotropy of the 1mm-thick AA6022-T4 aluminum alloy was probed with uniaxial tension experiments in 7 orientations to the RD, 3 plane-strain tension experiments at RD, 45° and TD and 1 disk compression experiment [3]. These experiments were fitted using the Yld2000-2D yield function [4] at a plastic work level of 27 MJ/m³ (or 10.6% strain in RD tension), Figure 1. The predicted R-values match the anisotropy found in the experimental R-values well, both showing a



minimum value at 45° to the RD, Figure 2. To calibrate the model shown in Figure 1, eight anisotropic fitting coefficients needed to be optimized and identified to describe the Yld2000-2D surface, Table 1. The governing parameters were optimized to fit the experimentally acquired stress states and R-values with an unconstrained nonlinear optimization code. Additionally, the strain hardening behavior of the material beyond the point of maximum uniform elongation (true $\varepsilon_{max} \approx 0.18$) was identified using a special case of the virtual fields method [5]. The Voce model was identified up to a plastic equivalent strain of about 0.3, see Figure 3.

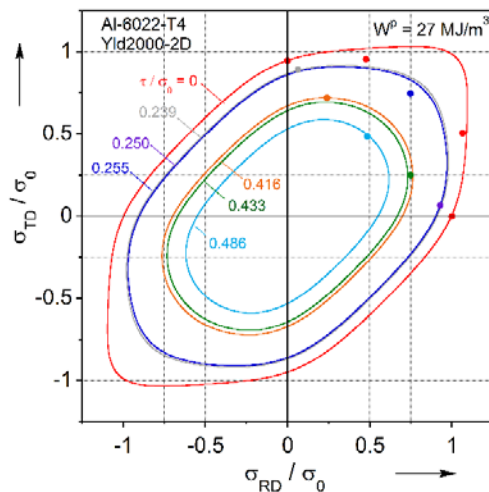


Figure 1. Normalized plane-stress yield locus (experiments and Yld2000-2D fit).

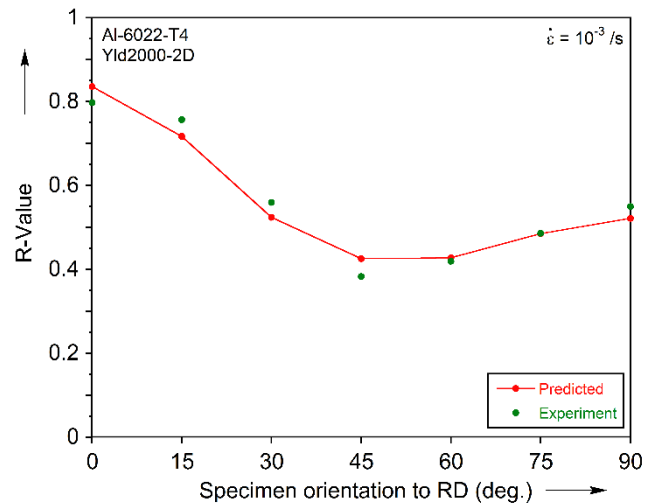


Figure 2. R-values obtained from experiments and predicted by Yld2000-2D at 27 MJ/m³.

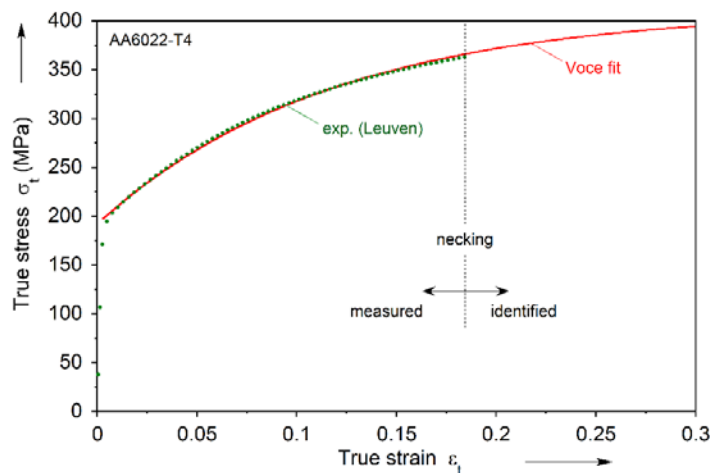


Figure 3. The true sts-strn curve of the material in the rolling direction. Inversely identified Voce law using experimental data beyond the point of maximum uniform strain (≈ 0.18).

Table 1.
Anisotropic coefficients used to fit Yld2000-2D ($W^p = 27 \text{ MJ/m}^3$).

k	8
α_1	0.9751
α_2	0.9998
α_3	0.9695
α_4	1.0669
α_5	0.9981
α_6	0.9323
α_7	0.9403
α_8	1.1572

3. Hole-expansion Experiments

The hole-expansion experiments were performed on a 260kN double-action hydraulic press with 305mm of stroke and with the same punch and die geometry as for a Marciniak test, Figure 4 (see also [3]). The specimen was clamped at the periphery by a lock-bead to prevent flow. The punch was then lowered onto the sheet with a speed of 1.065mm/s, until specimen failure was observed. The cup

height was approximately 19 mm at failure. A single crack was observed to propagate initially at 45° to RD of the sheet, Figure 5. To capture the evolution of strain in the specimen, a coat of matte white paint was applied to the surface of the specimen followed by a random black speckle pattern. The Correlated Solutions digital image correlation (DIC) VIC-3D software was used to analyze the images.

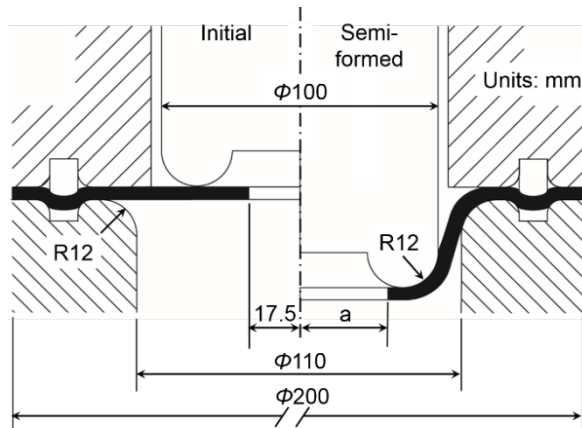


Figure 4. Punch and die geometry used for the hole-expansion experiments.



Figure 5. Specimen after experiment showing failure at 45° to the RD.

The three principal strains are shown in the last image captured prior to failure, at a punch displacement of approximately 19mm. The major and minor strains have the greatest absolute values along one of the 45 degree directions. Examining the third principal strain, i.e., the through thickness strain, it can be seen that thinning is also greatest along both 45° directions, Figure 6. That strain was determined from the two in-plane ones, using the incompressibility condition.

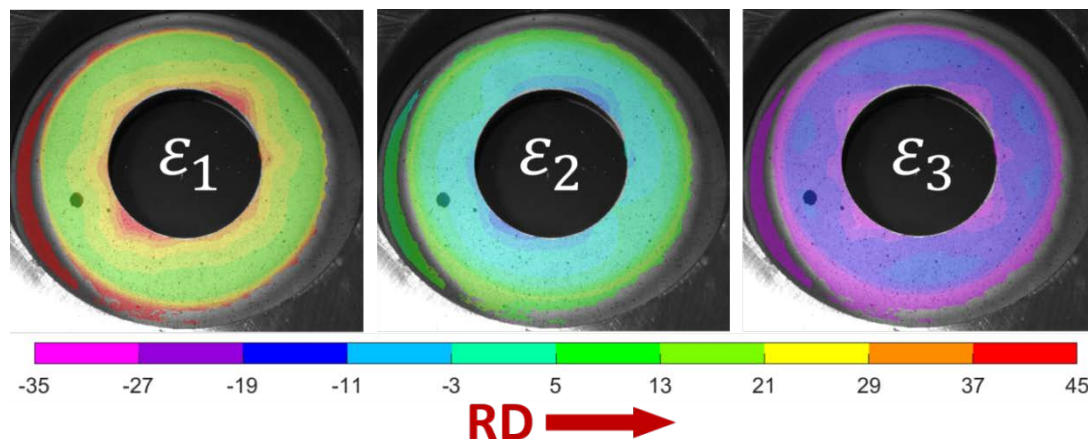


Figure 6. Principal strains shown immediately before failure is observed.

4. Hole-expansion Simulations

The hole-expansion of AA6022-T4 sheets was simulated using the explicit finite element code DYNAFORM. A quarter model was used due to the axisymmetric punch and die geometry and the fact that the R-values show 2-fold symmetry in the sheet. The mesh used 6,391 Belytschko-Tsay quadrilateral shell elements with 5 integration points through the thickness. To increase computational efficiency, the equivalent drawbead built into DYNAFORM is used to prevent the sheet flow past the drawbead. A friction coefficient of 0.17 between die and blank, punch velocity of 1000mm/s and time

step size of 1.2×10^{-6} were used. It can be seen in Figure 8 that the experimental and predicted thickness change values are in phase with each other, and generally have comparable mean values, but in every case they have drastically different amplitudes.

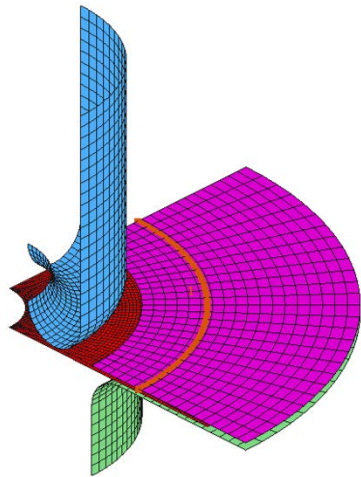


Figure 7. Finite element model used to simulate hole-expansion experiments using DYNAFORM

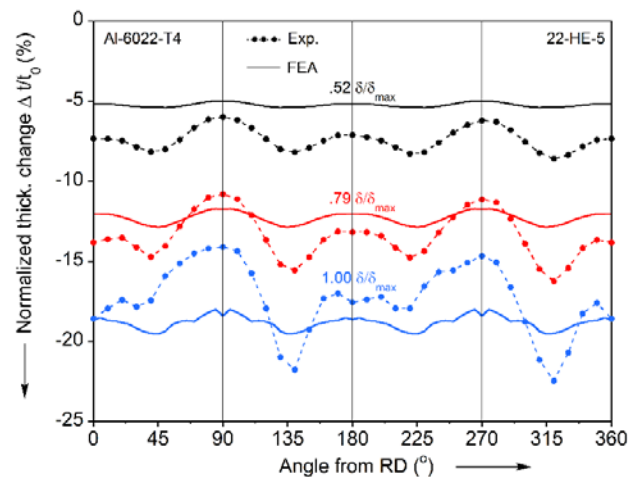


Figure 8. Evolution of experimental and FEA thickness change around the expanding hole at a fixed undeformed radius of 20mm at 3 normalized punch displacements.

5. Conclusions

The experimental data from the hole-expansion of AA6022-T4 sheets proved to be difficult to match using shell elements. This was despite the fact that the Yld2000-2D yield function, calibrated at 27 MJ/m³, matched the plasticity experiments very well and that the post-necking hardening curve was identified with a custom, dedicated procedure. The simulations reproduced the wavelength, but not the amplitude of the thickness variation around the circumference of the hole. To further improve the predictions, solid finite element models will be considered, along with material model calibrations at higher levels of plastic work.

References

- [1] Parmar, A., and Mellor, P.B. Plastic Expansion of a Circular Hole in Sheet Metal Subjected to Biaxial Tensile Stress. *Int. J. Mech. Sci.* 20.10 (1978): 707-20.
- [2] Kuwabara, T., Hashimoto, K., Iizuka, E. and Yoon J.W. Effect of Anisotropic Yield Functions on the Accuracy of Hole Expansion Simulations. *J. Mat. Proc. Tech.* 211.3 (2011): 475-81.
- [3] Tian, H., Brownell, B., Baral, M. and Korkolis, Y.P. Earing in Cup-Drawing of Anisotropic Al-6022-T4 Sheets. *Int J Mater Form* (2016): n. pag.
- [4] Barlat F, Brem JC, Yoon JW, Chung K, Dick RE, Lege DJ, Pourboghrat F, Choi S-H, Chu E (2003) Plane Stress Function for Aluminum Alloy Sheets-Part I: Theory. *Int J Plast* 19:1297–1319.
- [5] Coppieters, S., Cooreman, S., Sol, H., Van Houtte, P. and Debruyne, D. Identification of the Post-necking Hardening Behaviour of Sheet Metal by Comparison of the Internal and External Work in the Necking Zone. *J. Mat. Proc. Tech.* 211.3 (2011): 545-52.

Acknowledgements

This research was partially supported by the U.S. NSF GOALI grants CMMI-1031169 and CMMI-1301081. Prof. Haobin Tian acknowledges the support of National Natural Science Foundation of China (Grant No. 51405284). The AA6022-T4 sheets were provided by Dr. Edmund Chu of Alcoa.